

Radiation Efficiency Improvement of Zeroth-Order Resonator Antenna

David VRBA, Milan POLÍVKA

Dept. of Electromagnetic Field, Czech Technical University, Technická 2, 166 27 Praha, Czech Republic

vrbad1@fel.cvut.cz, polivka@fel.cvut.cz

Abstract. *The radiation as well as antenna efficiency of very thin profile zeroth-order resonator (ZOR) antenna, implemented in negative phase velocity (NPV) microstrip transmission line (TL) structure, has been solved by the method of moment simulator IE3D. The radiation is investigated using individual portions of the ZOR antenna that shows significant values of the surface current density. Dominantly radiating parts have been identified, geometrically emphasized by means of the increase in the antenna height over the ground plane from $1/105$ to $1/8 \lambda_0$. The measured parameters of the improved antenna prototype have been enhanced so they reached the following values (compared to original ones): gain 5.0 dBi (-3.0 dBi), antenna efficiency 97.7 % (9.5 %).*

Keywords

Antenna efficiency, electrically small antenna, metamaterial, negative phase velocity, radiation efficiency, zeroth-order resonator.

1. Introduction

The zeroth-order resonator (ZOR) implemented in a negative phase velocity (NPV), or also called composite right-left hand (CRLH) transmission line (TL), has been developed by several researchers and used to design electrically small antennas. The radiation and antenna efficiency have been, so far, rarely under investigation [1], [2], [3]. Relatively low values (ranging up to approx. 50 %) are reported [4]. In further design, the only antenna gain without a corresponding value of directivity and/or efficiency is provided [5].

Extremely low values of radiation efficiency do not enable the ZOR structures to work efficiently as an antenna. Therefore the question is whether the structure behaves rather as a lossy transmission line or as an antenna. As a result, the methods and techniques enabling to investigate the antenna and radiation efficiency of the antenna should be subjects of interest.

This paper presents the investigation of antenna and radiation efficiency of ZOR antenna implemented in a very thin NPV microstrip TL. In the paper, the numerical simu-

lation method of moment software IE3D [6] was used. The radiation is investigated from individual parts of the antenna structure (enabled in IE3D version 8). Dominantly radiating parts have been identified and geometrically emphasized by means of the increase in the height of the structure over the ground plane. The antenna efficiency of the improved (thick-substrate) ZOR antenna has been measured and compared with those of the original antenna (i.e. very thin-substrate antenna).

2. Negative Phase Velocity Phenomena

The concept of NPV phenomenon has been first comprehensively introduced by Veselago in 1968 [7]. In the aforementioned publication, he speculated on the existence of materials with a simultaneously negative permittivity (ϵ) and permeability (μ). He named these materials left-handed (LH) as \mathbf{E} , \mathbf{H} , and \mathbf{k} vectors of electromagnetic wave form a left-handed triad in case the wave propagates through such environment. He predicted unique electromagnetic properties of such materials as the reversal of Snell's law, the Doppler effect, and the Vavilov-Čerenkov effect. Although a possible implementation of NPV TL [8] appeared even before the Veselago work was published, it remained hidden for electromagnetic community for further three decades. The first experimental verification of NPV phenomena was performed by a research group at University of California, San Diego (UCSD) only in 2001 [9]. The LH material used in the above-mentioned verification consisted of metal split ring resonators (SRR) and a mesh of thin metal wires (MW). Later on, the concept of LHM was implemented in the planar transmission line (TL) technology [10], [11] via lumped capacitors and inductors periodically incorporated into the TL. This approach is considered more practical for series realizations.

2.1 Negative Phase Velocity in Transmission Line Implementation

NPV TL implemented in planar technology consists of TL with artificially inserted series capacitors C_L and shunt inductors L_L (with subscript L, denoting its left-handed properties). The equivalent circuit of the TL element can be then represented by four-lumped elements (as it is shown in Fig. 1).

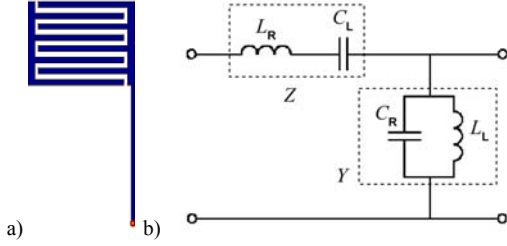


Fig. 1. Infinitesimal element of NPV TL a) and its equivalent circuit b) formed by inherent series inductor L_R and shunt capacitor C_R , artificially inserted series capacitors C_L and shunt inductor L_L .

The propagation constant of a TL is given by the relation $\gamma = \alpha + j\beta = \sqrt{ZY}$, where Z and Y stand for per-unit length impedance and per-unit length admittance, respectively. In the particular case of the CRLH TL, Z and Y are defined as follows

$$Z = j \left(\omega L_R - \frac{1}{\omega C_L} \right), \quad (1)$$

$$Y = j \left(\omega C_R - \frac{1}{\omega L_L} \right). \quad (2)$$

The dispersion relation for homogenous CRLH is then

$$\beta(\omega) = s(\omega) \sqrt{\omega^2 L_R C_R + \frac{1}{\omega^2 L_L C_L} - \left(\frac{L_R}{L_L} + \frac{C_R}{C_L} \right)} \quad (3)$$

where

$$s(\omega) = \begin{cases} -1 & \text{if } \omega < \omega_{\Gamma 1} = \min \left(\frac{1}{\sqrt{L_R C_L}}, \frac{1}{\sqrt{L_R C_R}} \right) \\ +1 & \text{if } \omega > \omega_{\Gamma 2} = \max \left(\frac{1}{\sqrt{L_R C_L}}, \frac{1}{\sqrt{L_L C_R}} \right) \end{cases} \quad (4)$$

In so-called balanced case [10], where

$$L_R C_L = L_L C_R \quad (5)$$

the phase velocity β reduces to

$$\beta = \beta_R + \beta_L = \omega \sqrt{L_R C_R} - \frac{1}{\omega \sqrt{L_L C_L}}. \quad (6)$$

Therefore, the electrical length or better phase shift $\theta = \beta l$ of the NPV TL of the length l can be either positive or negative, depending on the values of the equivalent circuit elements and the frequency range. The resonant length is then $l = |m|\lambda/2$ and the corresponding phase shift $\theta_m = \beta_m = (2\pi/\lambda)(m\lambda/2) = m\pi$, with $m = 0, \pm 1, \pm 2, \pm 3, \dots \pm \infty$. It means that the resonance index m is symmetrically defined around $m = 0$. For given values of lumped elements

of the equivalent circuit phase, the constant β equals to zero at the transition frequency ω_0 and is negative below ω_0 . Fig. 2, indicates the unbalanced case where propagation gap over f_0 ranges between 5.8 and 9.3 GHz.

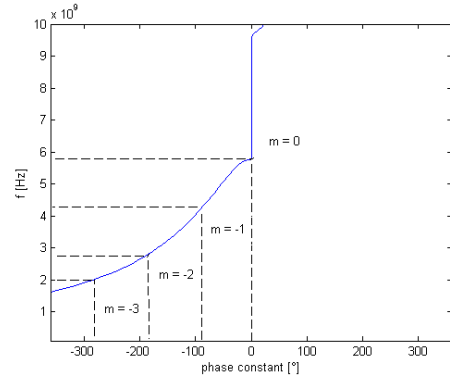


Fig. 2. Dispersion relation of NVP TL ($C_R = 0.52$ pF, $L_R = 1.8$ nH, $C_L = 0.15$ pF, $L_L = 1.45$ nH), unbalanced case with propagation gap within frequency band from 5.8 to 9.3 GHz.

2.2 Zeroth-Order Resonator

The phase constant $\beta = 0$ at ω_0 implies the infinite guided wavelength $\lambda_g = 2\pi/|\beta| = \infty$, and zero phase shift $\theta_m = -\beta l = 0$. This phenomenon enables the realization of zeroth-order resonance [10] in case that the length of the resonator is independent of the resonance condition (i.e. the multiple of the half wavelength in case of the open-circuited TL). The principal voltage distribution along the resonant length for the negative and zero resonances is shown in Fig. 3. A more comprehensive description of NPV TL implementation and ZOR properties can be found in [10].

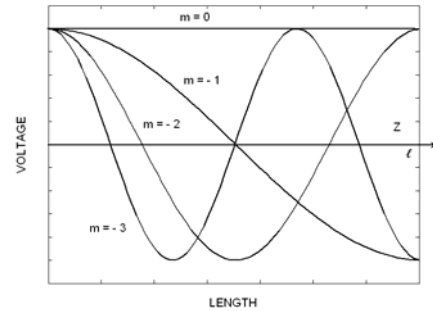


Fig. 3. Voltage distribution in case of open-circuited TL of length l . Mode $m = 0$ represents zeroth-order resonator with infinite guided wavelength.

NPV TL can thus form, if short enough, an electrically small zeroth-order resonator (ZOR) antenna, in case that sufficient radiation is enabled.

3. Zeroth Order Resonator Antenna

The efficient operation of a ZOR antenna is viable only in case that the antenna is impedance-matched and

provides sufficient radiation efficiency. The latter depends on the antenna physical size and the particular distribution of the current density on the antenna structure. In this paper, efficiency is investigated from the individual parts of the ZOR antenna structure that is implemented on the thin substrate ($h = 0.5$ mm) as NPV TL. In the literature, in case of the described ZOR antenna [5] a meander line forming shunt inductance L_L is used. The mirror current on the ground plane (below horizontal strips) has opposite orientation (phase) to the strip currents. In such a case, the contribution from the current elements flowing in the opposed direction is eliminated. Consequently, the significant drop in the radiation can be supposed for a very thin-substrate antenna. So the increase in the strip distance over the ground plane (GND) together with the use of the straight inductive stubs is supposed to enhance the radiation. Owing to that three prototypes have been designed. To compare their antenna efficiencies, the first of them was implemented on a very thin substrate ($h = 0.5$ mm, $\sim 1/105 \lambda_0$), while the second and third ones were designed using the increased height ($h = 6.9$ mm, $\sim 1/8 \lambda_0$). While the second one uses the same substrate as the first one, the third one was set up from dielectric substrate (0.5 mm) and air layer (6.4 mm).

3.1 Description of ZOR Antenna Structure

The original thin-substrate ZOR antenna with four element cells (see Fig. 4) has been designed in simulator IE3D with ZOR frequency $f_0 = 5.64$ GHz. The dielectric substrate GML 1000 ($h = 0.5$ mm, $\epsilon_r = 3.05$, $\tan\delta = 0.003$) was used. The physical dimensions of the original antenna prototype are $12.0 \times 4.9 \times 0.5$ mm which represents a relative size $1/5 \times 1/11 \times 1/105 \lambda_0$. The ground plane size is 60.0×40.0 mm, which is $1.1 \times 0.75 \lambda_0$. In the simulation here, the ground plane is considered infinite. The antenna was excited by a coaxial feeder of the diameter r_1 . The series capacity of the equivalent circuit model (Fig. 1) was implemented as interdigital capacitor. As a parallel inductance a straight strip, connected by via hole to the ground plane, has been used. In this case, the overall length of one single basic cell is $p = 3$ mm; the length of fingers of interdigital capacitors equals $l_{ind} = 2.5$ mm and the width of the finger w is the same as the width of the gap s , i.e. $w = s = 0.1$ mm. The equivalent circuit model of the cell corresponds to the schema depicted in Fig. 1. The values of interdigital capacitor C_L and inductive stub L_L can be calculate according to [13] as

$$C_L = 1/3(n-1)(\epsilon_r + 1)\epsilon_0(\ln(1 + w_p/s) + 3/4), \quad (7)$$

$$L_L = \frac{Z_V}{\omega} \operatorname{tg}kl \quad (8)$$

where n is the number of interdigital arms, w_p is the width of the finger, and s is the width of the gap between fingers. At first, we simulated s-parameters of the unit cell in IE3D. To find the values of series inductance L_R and parallel capacitance C_R we fitted the values of simulated s-para-

eters from IE3D to the values of s-parameters acquired from the circuit model of the unit cell implemented in AWR Microwave Office. The value of equivalent elements at $f_0 = 5.64$ GHz then accounts for $C_R = 0.52$ pF, $L_R = 1.8$ nH, $C_L = 0.15$ pF, $L_L = 1.45$ nH. The cell has been designed as unbalanced so that it is possible to realize the circuit elements in the microstrip technology. The EM model cell shows slightly different resonant values than those calculated from the circuit model because of the simplicity (the lossless model and no coupling are considered).

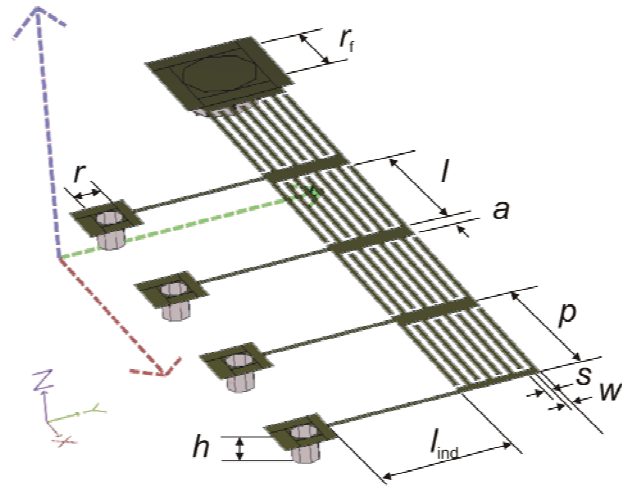


Fig. 4. Model of 4 unit cell ZOR antenna with substrate GML 1000 ($\epsilon_r = 3.05$, $\tan\delta = 0.003$) of height $h = 0.5$ mm with infinite ground plane (not shown).

3.2 Radiation from Selected Parts of Antenna

As it can be seen in Fig. 5, the magnitude of the surface current density flowing on the horizontal strips of shunt inductors exceeds its values existing on the rest of the structure by at least 10 dB. The above-mentioned strips thus form source areas that radiate significantly.

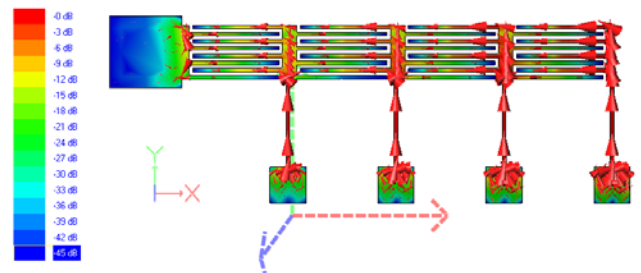


Fig. 5. Vector current distribution at zeroth order resonance frequency $f_0 = 5.64$ GHz.

For the investigation of the radiation of the ZOR antenna the current distribution of the whole antenna and also selected antenna regions (denoted in Fig. 6 by dashed red rectangles) is used. The relative drop-off of the radiation of selected regions to the radiation of the whole antenna structure can be observed in four cases, see Fig. 7 and 8. The aforementioned drop-off is evaluated and the domi-

nantly radiating parts are identified. In the improved version of ZOR antenna, these parts (namely horizontal strips

and vertical pins) are then geometrically emphasized by a rise in the antenna height over the ground plane.

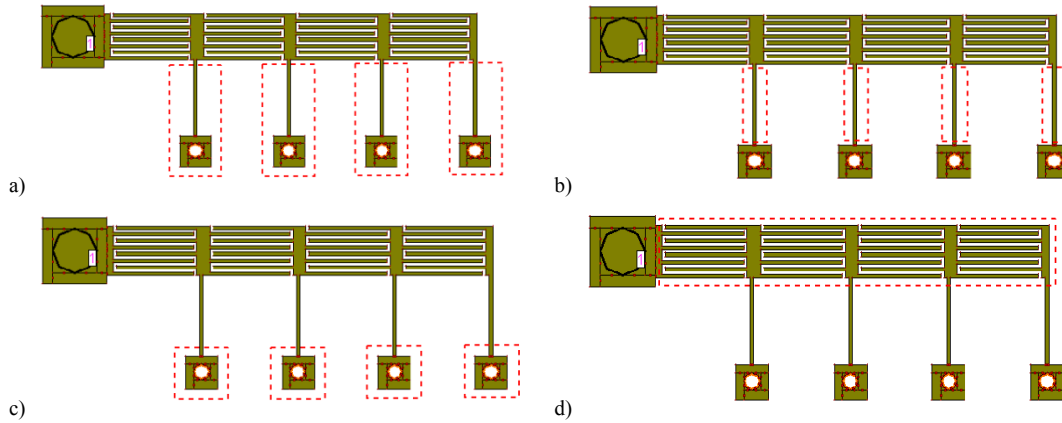


Fig. 6. Picture of antenna footprint with selected regions: a) horizontal strips and vertical vias of shunt inductors, b) horizontal strips solely of shunt inductors, c) vertical vias solely of shunt inductors, d) series capacitors

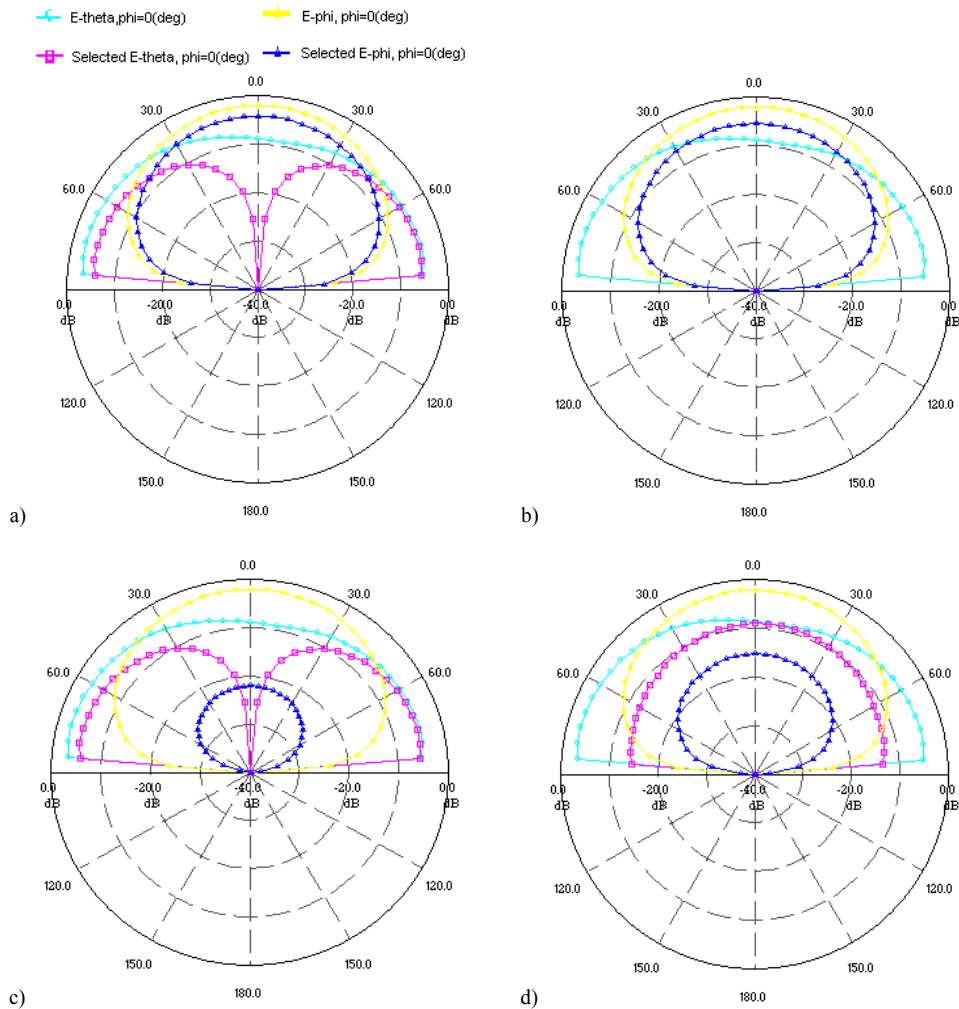


Fig. 7. Radiation pattern from both, total structure and selected regions of the original ZOR antenna design ($h = 0.5$ mm) in $\varphi = 0^\circ$ plane: a) horizontal strips and vertical vias of shunt inductors, b) horizontal strips solely of shunt inductors, c) vertical vias solely of shunt inductors, d) series capacitors.

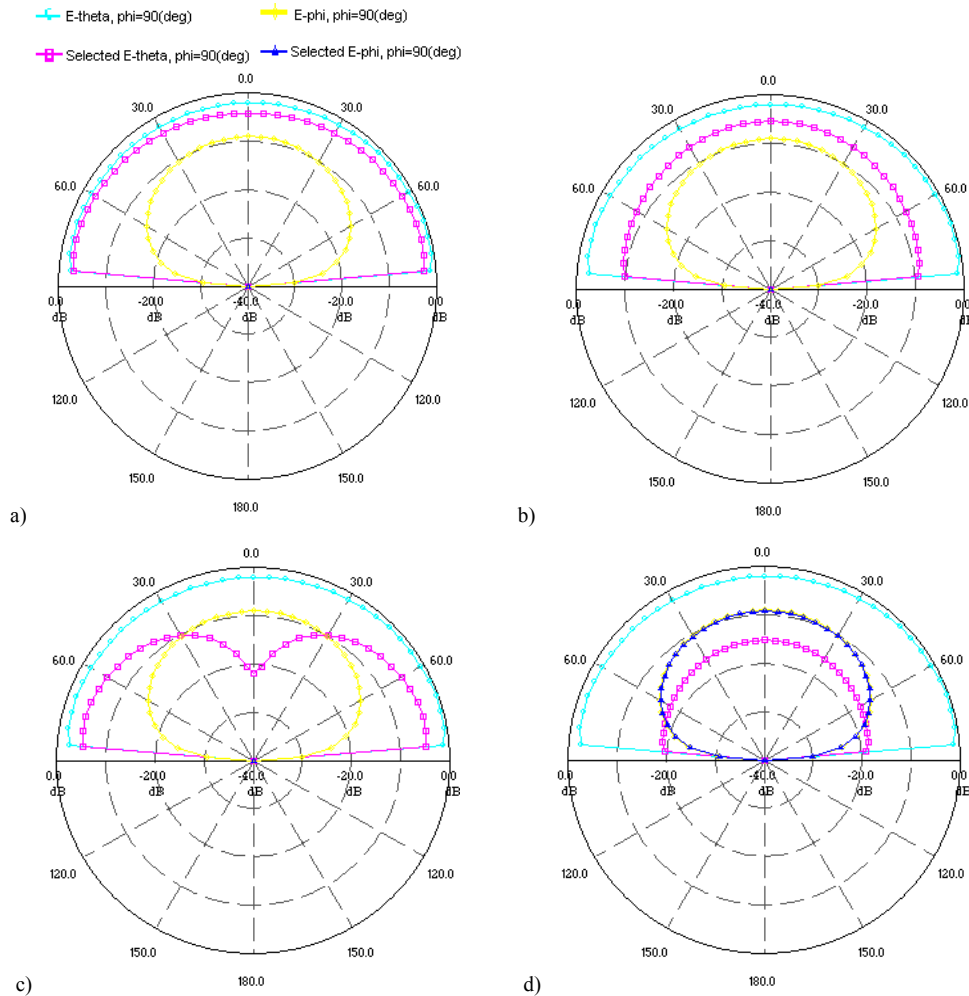


Fig. 8. Radiation pattern from both total structure and selected regions of original ZOR antenna design ($h = 0.5 \text{ mm}$) in $\varphi = 90^\circ$ plane: a) horizontal strips and vertical vias of shunt inductors, b) horizontal strips solely of shunt inductors, c) vertical vias solely of shunt inductors, d) series capacitors.

First, let us comment on the radiation pattern components in the $\varphi = 0^\circ$ plane (xz plane) and then in $\varphi = 90^\circ$ (yz plane) plane. We always compare the magnitudes of the E-field components from the whole structure (e.g. $E_\theta(\varphi = 0^\circ)$ or $E_\varphi(\varphi = 0^\circ)$) and from the selected regions (e.g. Selected $E_\theta(\varphi = 0^\circ)$ or Selected $E_\varphi(\varphi = 0^\circ)$). As it is evident from the comparison of $E_\varphi(\varphi = 0^\circ)$ (yellow line) and Selected $E_\varphi(\varphi = 0^\circ)$ (dark blue line) components in Fig. 7b, the horizontal strips of the shunt inductors significantly contribute to the radiation in the whole upper hemisphere. From the comparison of $E_\theta(\varphi = 0^\circ)$ (light blue line) and Selected $E_\theta(\varphi = 0^\circ)$ (violet line) components in Fig. 7c, it is obvious that the significant radiation contribution into the directions out of normal comes from the vertical vias of the shut inductors, whereas in case of the direction of normal, it comes from the series capacitors (see Fig. 7d). The comparison of $E_\theta(\varphi = 90^\circ)$ (light blue line) and Selected $E_\theta(\varphi = 90^\circ)$ (violet line) components in Figs. 8b and 8c shows similar results as the previous comparison of $E_\varphi(\varphi = 0^\circ)$ and Selected $E_\varphi(\varphi = 0^\circ)$ components in $\varphi = 0^\circ$ plane.

According to the literature [1-5] the value of the radiation efficiency of ZOR antennas (manufactured using a thin dielectric substrate) usually does not exceed 50 %. The frequency dependence of the efficiencies of the original thin-substrate antenna ($h = 0.5 \text{ mm}$) is less than 10 %; see Fig. 9. The efficiencies presented in this paper are defined in the following way:

$$\begin{aligned} \text{Radiation efficiency} &= \text{Radiated Power}/\text{Input Power} \\ \text{Antenna efficiency} &= \text{Radiated Power}/\text{Incident Power}. \end{aligned}$$

The supposed way how to improve the radiating efficiency is to increase the height of the NPV TL over the ground plane. This measure is taken in order to increase the distance of the currents flowing on the horizontal strips of inductive stubs over their mirror out-phase currents that are induced on the ground plane. The improved antenna thus has an additional air layer between the ground plane and the thin dielectric substrate carrying the antenna motif. The height of the air layer is, due to the available foam spacers, chosen $h_{air} = 6.4 \text{ mm}$ ($\sim 1/9 \lambda_0$), so that the total height equals to $h = h_{diel} + h_{air} = 0.5 + 6.4 = 6.9 \text{ mm}$. The fre-

quency dependence of the efficiencies of the improved antenna is depicted in Fig. 10. To properly take into account for the presence of dielectric between the antenna layer and ground plane the simulated results of efficiencies for an antenna designed on a thick ($h = 6.9$ mm) substrate are presented in Fig. 10. As it can be seen radiation efficiency has been improved from 10 % to about 30 %. Further improvement of radiation efficiency up to more than 80 % can be reached by decreasing of relative permittivity below the antenna motif – removing the dielectric which is substituted by an air of thickness 6.4 mm, see Fig.11.

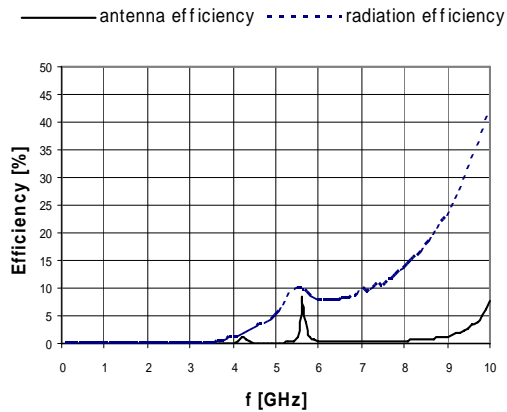


Fig. 9. Simulated radiation and antenna efficiency of original thin antenna ($h = 0.5$ mm) with infinite ground plane.

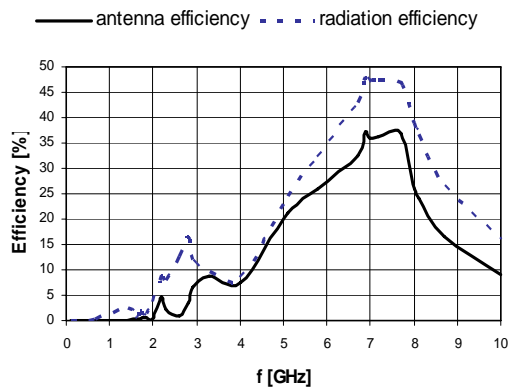


Fig. 10. Simulated radiation and antenna efficiency of thick profile antenna ($h = 6.9$ mm, full substrate) with infinite ground plane.

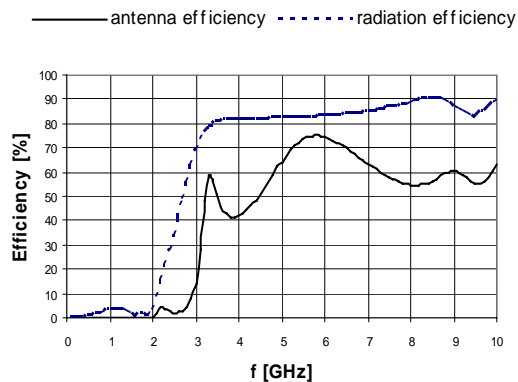


Fig. 11. Simulated radiation and antenna efficiency of the improved antenna ($h = 6.9$ mm with air layer of thickness 6.4 mm) with infinite ground plane.

4. Results

Given the measured and simulated frequency behavior of the reflection coefficient S_{11} , it is apparent that for the original thin-substrate antenna, the shapes and minima of the above-mentioned curves are almost identical (see Fig. 13). On the contrary, for the improved antenna the measured reflection coefficient exhibits two sharp minima around the simulated zeroth order resonance (Fig. 14). This effect can be caused by several reasons, e.g. by the fabrication tolerance (see the photograph of the manufactured prototype in Fig. 12) or resonance of finite sized ground plane. Simulation of original and improved antennas has also been performed with finite ground plane to make the comparison of directivity and gain of simulated and measured antennas more precise.

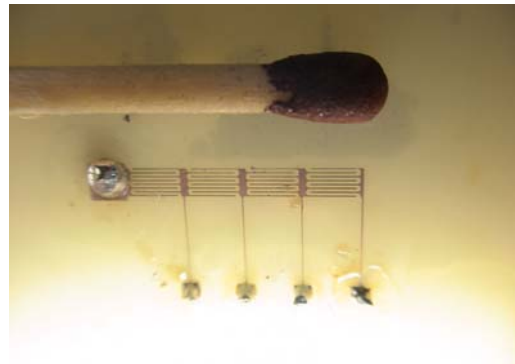


Fig. 12. Photograph of the improved antenna.

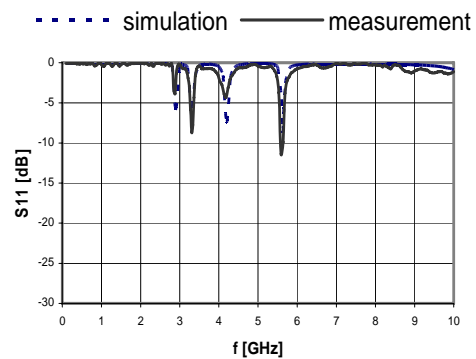


Fig. 13. Measured and simulated reflection coefficient of realized prototype of the original antenna with infinite ground plane.

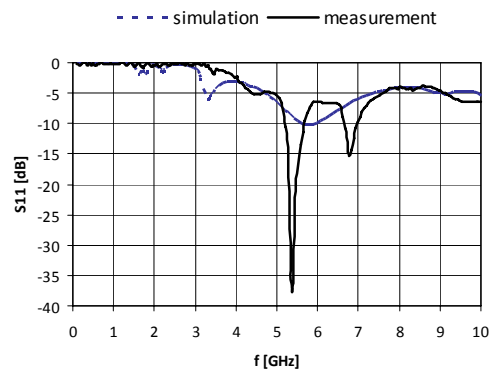


Fig. 14. Measured and simulated reflection coefficient of the realized prototype of the improved antenna with infinite ground plane.

Directivity, gain, and efficiency of both original and improved air dielectric substrate antennas with infinite ground plane have been simulated, see Tables 1 and 2.

m	-3	-2	-1	0
f_m [GHz]	2.90	3.30	4.20	5.63
G [dBi]	-39.3	-31.5	-14.7	-6.0
D [dBi]	6.5	7.1	4.1	5.0
η [%]	0.0	0.0	1.2	7.9

Tab. 1. Simulated values of gain G , directivity D and efficiency η of the original antenna with infinite ground plane for negative and zero resonances.

m	-3	-2	-1	0
f_m [GHz]	1.80	2.20	3.30	5.80
G [dBi]	-18.0	-8.9	4.0	4.4
D [dBi]	5.6	4.4	6.4	5.7
η [%]	0.4	4.7	57.5	74.1

Tab. 2. Simulated values of gain G , directivity D and efficiency η of the improved antenna with infinite ground plane for negative and zero resonances.

Simulated and measured parameters of both, the original and the improved antennas now with finite ground plane are presented in Tab. 3.

Antenna (finite ground plane)	Original		Improved	
	Sim.	Meas.	Sim.	Meas.
f_0 [GHz]	5.60	5.64	5.80	7.79
G [dBi]	-3.0	-4.5	4.0	5.0
D [dBi]	5.8	5.7	4.5	5.1
η [%]	13.2	9.5	89.1	97.7

Tab. 3. Measured gain G , calculated directivity D , and calculated efficiency η of the original and improved antennas at f_0 realized with finite ground plane.

Measured radiation patterns of both antennas with finite ground plane are presented in Fig. 15 and Fig. 16.

5. Summary

The radiation of the very thin profile ZOR antenna implemented in NPV TL has been investigated from selected regions of the antenna. The objective was to find the dominantly radiating source areas. It has been found that these areas are formed by the horizontal strips and vertical vias of LH inductors. Given these findings, an efficiency improved ZOR antenna with air substrate and increased vertical height from 0.5 mm to 6.9 mm, which represent relative increase of height from $1/105$ to $1/8 \lambda_0$ has been designed and measured. The simulated 6.9 mm thick full dielectric substrate antenna provides just partial improvement of radiation efficiency from about 10 to 30 % at f_0 . Further improvement, maintaining the antenna height, up to more than 80 % can be reached by decreasing the relative permittivity of substrate layers below the antenna motif. The simulated antenna efficiency of finite ground

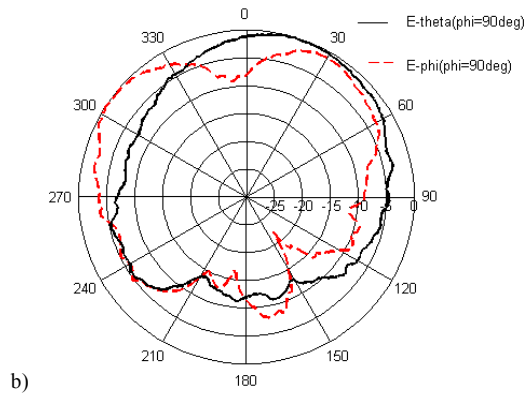
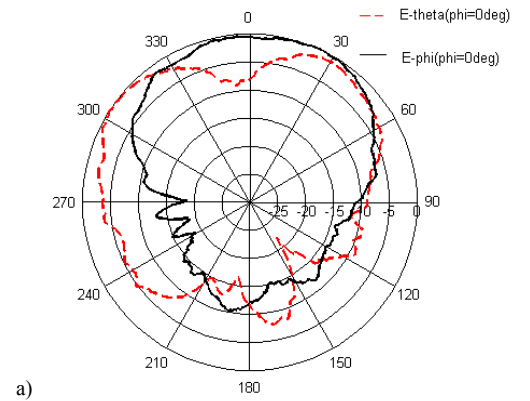


Fig. 15. Radiation patterns of original (thin profile) antenna a) $\phi = 0^\circ$ (xz plane), b) $\phi = 90^\circ$ (yz plane).

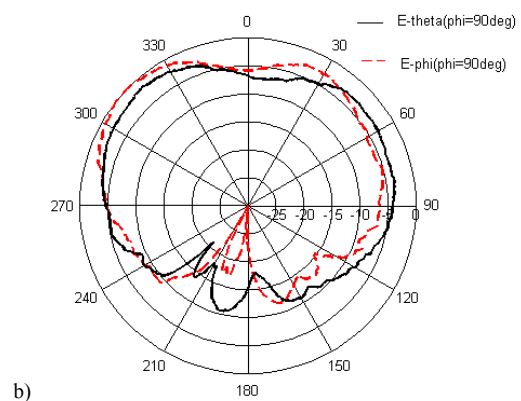
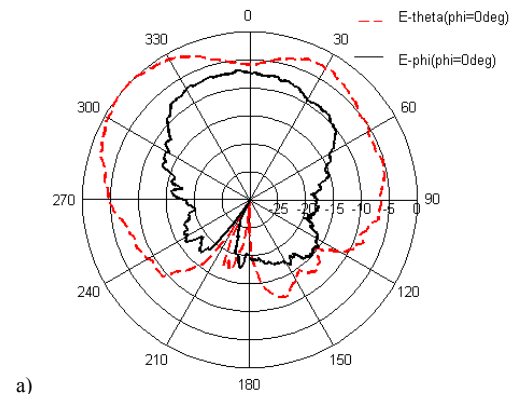


Fig. 16. Radiation patterns of improved (increased profile) antenna a) $\phi = 0^\circ$ (xz plane), b) $\phi = 90^\circ$ (yz plane).

plane air substrate antenna has been increased from 13.2 to 89.1 %, while the measured one has been increased from 9.5 to 97.7 %. The measured gain has been enhanced from -4.5 to 5.0 dBi. The increased height of vertical vias of the improved antenna changes a shape of the radiation pattern which is more similar to the monopole antenna one, see Fig. 15 and Fig. 16 where component values denoted by red dashed curve dominates.

To sum it up, it can be stated that the radiation efficiency (and consequently also the antenna efficiency) depends predominantly on the vertical size of the antenna structure and as much low relative permittivity as possible. The height of the here presented improved (thick profile) ZOR antenna is as far as half of a monopole antenna height and there is a question to be solved if the use of such ZOR antenna may provide any significant advantages compared to the monopole one.

Acknowledgements

The research was conducted at the Department of Electromagnetic Field of the Czech Technical University in Prague and supported by the Czech Science Foundation within two projects - No. 102/08/1282 "Artificial electromagnetic structures for miniaturization of high-frequency and microwave radiation and circuit elements", and also within the doctoral project No. 102/08/H018. In addition, it gained support from the Czech Ministry of Education, Youth and Sports within the Research Project in the Area of the Prospective Information and Navigation Technologies MSM 6840770014, and also the COST project IC0603 "Antenna Systems & Sensors for Information Society Technologies".

References

- [1] SCHÜSSLER, M., OERTEL, M., FRITSCHÉ, C., FREESE, J., JAKOBY, R. Design of periodically L-C loaded patch antennas. In *27th ESA Antenna Technology Workshop on Innovative Periodic Antennas*. Santiago de Compostela (Spain), March 2004.
- [2] SCHÜSSLER, M., FREESE, J., JAKOBY, R. Design of compact planar antennas using LH-transmission lines. In *IEEE MTT-S International Microwave Symposium Digest*, 2004, pp. 209-212.
- [3] SANADA, A., KIMURA, M., AKAI, I., KUBO, H., CALOZ, C., ITOH, T. A planar zero-th order resonator antenna using left-handed transmission line. In *Proc. of European Microwave Conference* (CD ROM). Amsterdam (the Netherlands), 2004.
- [4] QURESHI, F., ANTONIADES, M. A., ELEFTERIADES, G. V. A compact and low-profile metamaterial ring antenna with vertical polarization. *IEEE Antennas and Wireless Propagation Letters*, vol. 4, 2005, p. 333-336.
- [5] PARK, J.-H., RYU, Y.-H., LEE, J.-G., LEE, J.-H. A zeroth-order resonator antenna using epsilon negative meta-structured transmission line. In *Proc. of IEEE Antennas and Prop. Symposium* (CD ROM). Honolulu (Hawaii), 2007.
- [6] Inc. Zeland Software. *IE3D 11.5 Users Manual*. Zeland Software, Inc., 39120 Argonaut Way, Suite 499, Fremont, CA 94538, U.S.A., October 2005.
- [7] VESELAGO, V. The electrodynamics of substances with simultaneously negative values of ϵ and μ . *Soviet Physics Uspekhi*, vol. 10, no. 4, Jan., Feb. 1968, pp. 509-514.
- [8] MALYUZHINETS, G. D. A note on the radiation principle. *Zhurnal technicheskoi fiziki*, vol. 21, 1951, pp. 940-942 (in Russian).
- [9] SHELBY, R. A., SMITH, D. R., SCHULTZ, S. Experimental verification of a negative index of refraction. *Science*, vol. 292, April 2001, pp. 77-79.
- [10] CALOZ, C., ITOH, T. *Electromagnetic Metamaterials: Transmission Line Theory and Microwave Applications*. John Wiley & Sons, 2006.
- [11] ELEFTERIADES, G. V., IYER, A. K., KREMER, P. C. Planar negative refractive index media using periodically L-C loaded transmission lines. *IEEE Trans. Microwave Theory Tech.*, vol. 50, no. 12, 2002, pp. 2702-2712.
- [12] VRBA, D. *Electrically Small Antenna with Lumped LC Elements* Master thesis, CTU FEE, 2008.
- [13] SVAČINA, J. *Investigation of Microwave Planar Structures Using the Conformal Mapping Method*. Brno: Akademické nakladatelství CERM, 2006 (in Czech).

About Authors...

David VRBA graduated from the Czech Technical University in Prague in 2008. He currently works towards his Ph.D. degree. In his research, he specializes in the field of metamaterials and antennas.

Milan POLÍVKA received his M.Sc. degree from the Czech Technical University in Prague in 1996. In the same year, he joined the Department of Electromagnetic Field and was appointed an assistant professor. In 2003, he received his Ph.D. degree in Radio Electronics from the same department. The fields of his research interest are antennas, artificial electromagnetic materials and RFID systems. He is a member of IEEE. Since 2007 he serves a Chair of the MTT/AP/ED/EMC Joint Chapter of Czechoslovakia section of IEEE.